05

Stimulated emission in $Al_2O_3/AlN/Al_{0.65}Ga_{0.35}N/AlN/Al_2O_3$ heterostructure with symmetric planar waveguide

© P.A. Bokhan[1], D.E. Zakrevsky[1,2], T.V. Malin[1], N.V. Fateev[1]

[1] Rzhanov Institute of Semiconductor Physics, Siberian Branch, Russian Academy of Sciences, Novosibirsk, Russia
[2] Novosibirsk State Technical University, Novosibirsk, Russia

e-mail: fateev@isp.nsc.ru

Received December 12, 2025
Revised December 12, 2025
Accepted February 24, 2026

The properties of stimulated emission in a symmetric $Al_2O_3/AlN/Al_{0.65}Ga_{0.35}N/AlN/Al_2O_3$ heterostructure were experimentally studied in the spectral range $\lambda = 350-700$ nm at room temperature. The active medium is a symmetric planar waveguide formed by two identical heavily doped $Al_{0.65}Ga_{0.35}N/AlN/Al_2O_3$ structures, with their active layers tightly pressed together. The emission was coupled out through the side surface (leaky modes) and through the end face of the structure (guided modes). When optically pumped with $\lambda = 266$ nm, the structure exhibits amplifying properties with an optical gain of $g \sim 41\,cm^{-1}$ at a pump power density of $P_p = 460\,kW/cm^2$. The stimulated emission spectrum is a broad band containing peaks due to the mode structure of the emission and the excitation of orthogonally polarized waveguide TE and TM modes. The quantum efficiency of the stimulated emission output is $\eta \sim 20\,\%$. The angular divergence of the beam is 15° in the plane of the structure and 18° in the perpendicular direction.

Keywords: heavily doped $Al_xGa_{1-x}N$ structure, symmetric planar waveguide, optical gain, donor-acceptor recombination.

DOI: 10.61011/0000000000

Introduction

$Al_xGa_{1-x}N$ films, due to a number of their unique parameters, are a promising material in optoelectronics for creating radiation sources in the ultraviolet range of the spectrum [1]. Radiative recombination centers are formed in silicon-doped Si with a concentration of $n_{Si} \geq 1.5 \cdot 10^{20}\,cm^{-3}$ $Al_xGa_{1-x}N$ layers with $x > 0.5$ (see, for example, [2]). When excited by an electron beam and optical excitation, these structures are characterized by a continuous inhomogeneously broadened luminescence spectrum in the wavelength range of $\lambda = 350-750\,nm$, while the internal quantum yield of η exceeds 50% [3], and the luminescent characteristics are preserved up to the temperature of 400 °C. These parameters make it attractive to create broadband light-emitting sources and wavelength-tuning lasers in a wide spectral range based on them. The main mechanism of broadband radiation formation is donor-acceptor recombination with a radiative recombination cross-section of $\sigma \approx 10^{-15}$,cm^2 at a concentration of recombination centers of more than $\sim 10^{20}$,cm^{-3} [4]. In this case, large values of optical gain coefficients are realized $g \approx \sigma \cdot n_{Si} \sim 10^4\,cm^{-1}$. The contribution of electron-hole recombination to the broadband radiation spectrum is much smaller and amounts to less than 5% of the total intensity [5].

Typical structures with good optical quality of the active layer, studied in Ref. [6], were an asymmetric waveguide of the type „film $Al_xGa_{1-x}N$–buffer layer AlN–sapphire substrate Al_2O_3“. The thickness $Al_xGa_{1-x}N$ films usually did not exceed $h_0 \approx 1.2\,\mu m$. The growth of thick $h_0 > 2\,\mu m$ layers is complicated by the appearance of cracks in the cultivated layer [7]. The mechanism of crack formation is related to residual stresses in the epitaxial layers. It is known from the literature data that in the AlGaN:Si layers lateral stresses are compressive at $x < 0.4$, but for $x > 0.4$ they become tensile [8]. It has been experimentally established that in the $Al_xGa_{1-x}N$:Si/AlN/Al_2O_3 with $x > 0.5$ and the doping level $n_{Si} \sim 5.0 \cdot 10^{19}\,cm^{-3}$ and the total thickness of the epitaxial layer $h_0 \approx 1.5\,\mu m$, cracks are observed, which leads to a deterioration in the optical properties of the structures.

Increasing the size of the active medium by increasing the film thickness is one of the ways to increase the output power of stimulated radiation. The purpose of this work is to study the characteristics of stimulated emission (optical amplification, spectral and energy parameters) in a symmetrical planar waveguide, which makes it possible to increase the thickness of the active medium without growing the epitaxial layer above a critical value. The active medium uses a structure formed by two identical asymmetric heterostructures $Al_{0.65}Ga_{0.35}N/AlN/Al_2O_3$ with an active layer thickness of $h_0 \approx 1.1\,\mu m$ pressed against each other by active layers. This configuration forms a symmetrical planar waveguide with a sequence of layers $Al_2O_3/AlN/Al_{0.65}Ga_{0.35}N/AlN/Al_2O_3$ (Fig. 1).

A significant number of theoretical and experimental papers have been devoted to the study of the radiative characteristics of various structures in asymmetric planar

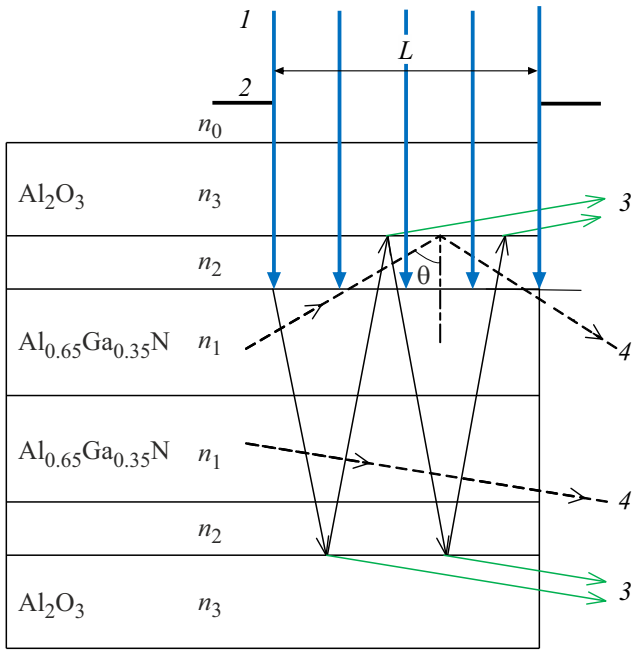


Figure 1. The scheme of excitation and registration of output radiation in the heterostructure $Al_2O_3/AlN/Al_{0.65}Ga_{0.35}N/AlN/Al_2O_3$: *1* —optical pumping, *2* — diaphragm, *3* — stimulated radiation from the resulting modes, *4* — stimulated radiation from the end of the waveguide (dashed line).

waveguides for various configurations (see, for example, [6,9–11]). In the case of symmetrical waveguides, the situation is different: the mainattention in the literature is paid to theoretical analysis, while experimentalstudies are presented significantly less (for example, [12,13]).

1. Experiment procedure

The object of the study is an active medium implemented in the form of a symmetrical planar waveguide. This structure was obtained by close mechanical contact of two identical asymmetric $Al_{0.65}Ga_{0.35}N/AlN/Al_2O_3$-heterostructure. Each of the initial structures consisted of an $Al_{0.65}Ga_{0.35}N$ film with a thickness of $h_0 \approx 1.1\,\mu$m and an AlN buffer layer with a thickness of $h_1 \approx 360$ nm grown on (0001) oriented nitrided sapphire substrates Al_2O_3 with a thickness of $h = 430\,\mu$m. The technology of synthesis of $Al_{0.65}Ga_{0.35}N/AlN/Al_2O_3$ heterostructures and measurement of their parameters are described in detail in Ref. [14]. As a result of the tight pressing of two such structures by active layers, a new symmetrical heterostructure was formed with a sequence of layers $Al_2O_3/AlN/Al_{0.65}Ga_{0.35}N/AlN/Al_2O_3$. The total thickness of the configuration core was $h_\Sigma = 2h_0 \approx 2.2\,\mu$m. All the studied samples were obtained by the method of mechanical cleavage of structures along the crystallographic planes of sapphire. The cross-cleavage images for $Al_2O_3/AlN/Al_{0.65}Ga_{0.35}N/AlN/Al_2O_3$-heterostructures are shown in Fig. 2.

The radiation parameters were studied under optical excitation from a sapphire film by radiation from the fourth harmonic of a pulsed Nd:YAG laser with $\lambda = 266$ nm with a pulse duration at half-height of 8 ns at a repetition frequency of 10 Hz. The pump radiation was focused on the surface of the structure by a cylindrical lens with a focal length of 5 cm, forming a homogeneous excitation zone with a width of $b \approx 100\,\mu$m and a length of $L = 0-5$ mm with an adjustable pitch of $5\,\mu$m. Under these conditions, the film $Al_{0.65}Ga_{0.35}N$ absorbed $\sim 75\,\%$ of the pump radiation [4]. The inhomogeneity of the pump radiation intensity along the pump band did not exceed 5,%. All experiments were performed at room temperature.

The luminescence spectra were measured at an angle of about 45° to the sample plane, and the stimulated radiation was — perpendicular to the end of the structure with a broadband spectrometer in the $\lambda = 250-800$ nm range with a resolution of 0.5 nm [15]. Part of the measurements of the values for radiation intensities were carried out at a fixed wavelength using a prism monochromator with a resolution of 10 nm and a photomultiplier FEU–106, the signal from which was recorded by a Tektronix TDS2024B oscilloscope. The radiation was transmitted through a quartz fiber with an inner diameter of 0.1cm to a spectrometer (Kolibri-2) and a monochromator (Carl Zeiss). The polarization characteristics of the output radiation were determined using

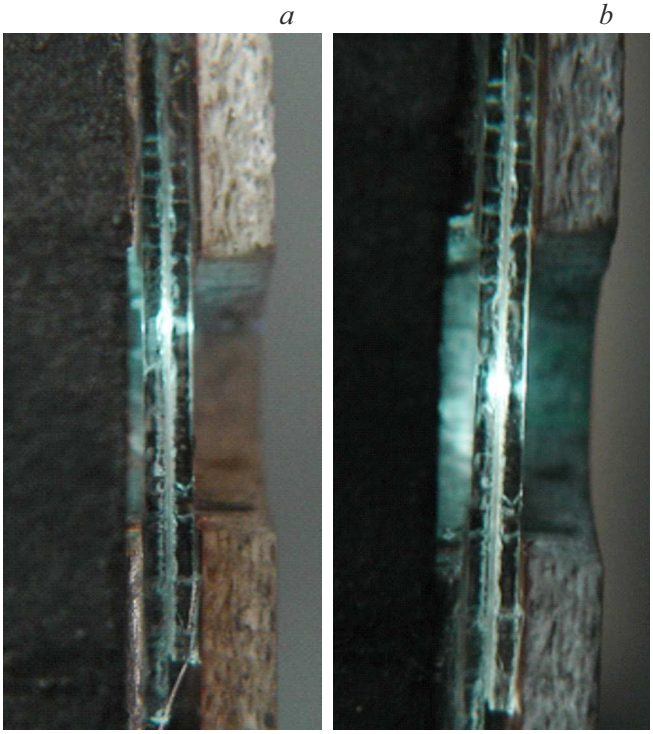


Figure 2. Images of the radiation spot and transverse cleavage of the $Al_2O_3/AlN/Al_{0.65}Ga_{0.35}N/AlN/Al_2O_3$ heterostructure at a pump power density of $P_p \approx 20$ kW/cm^2 (*a*) and 55 kW/cm^2 (*b*).

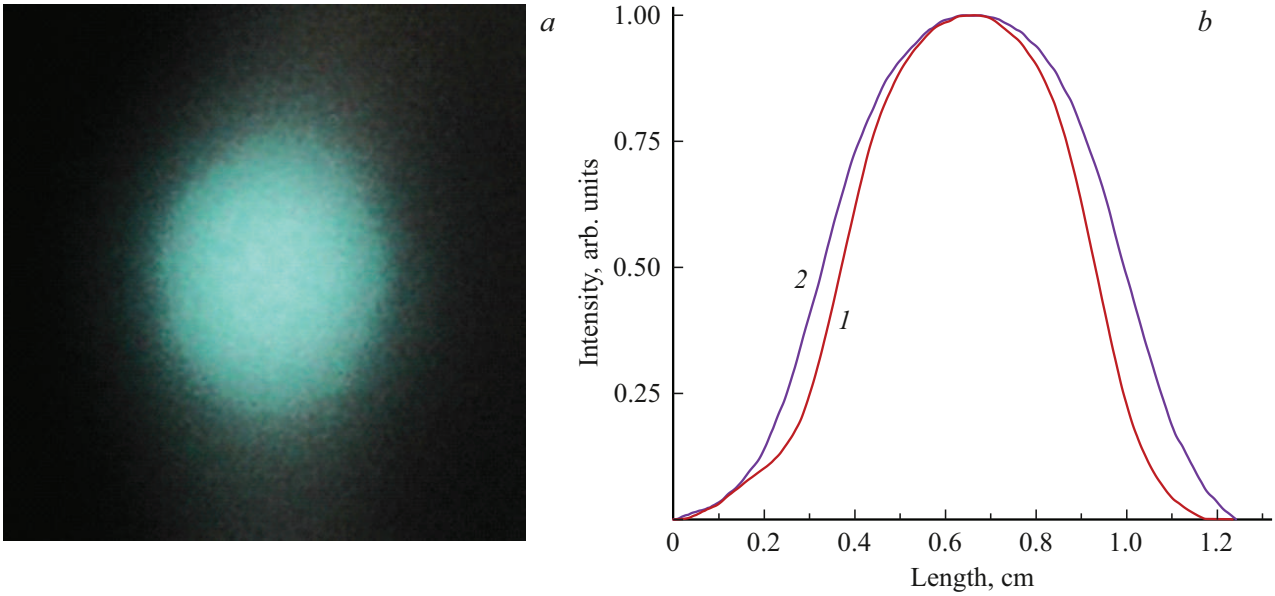


Figure 3. (*a*) A photograph of the output spot of stimulated radiation at a distance of 10 cm from the heterostructure. (*b*) Spatial distribution of the output beam intensity for two mutually perpendicular directions: *1* — horizontal (perpendicular to the surface of the structure), *2* — vertical (along the surface of the structure).

a Glan prism. The pumping and stimulated radiation powers were measured by a Thorlabs S401C sensor.

In experiments, the stimulated emission pattern was determined by the threshold character and exponential increase in the intensity of the output radiation with an increase in the length of the excitation zone L, with an increase in the pumping intensity, by the formation of the mode structure of the radiation spectrum and the output radiation spot with low divergence. In this case, in addition to a wide band, single spectral components are present in the radiation spectrum, which are formed due to the resulting modes. There is no narrowing of the width of the stimulated radiation line, since the luminescence spectrum is characterized by an inhomogeneous broadening of the radiation line [4].

2. Experimental results and discussion

Optical excitation of the structure leads to the appearance of broadband luminescence, and stimulated radiation appears at the optical pump power density $P_p > 6\,\text{kW/cm}^2$. Fig. 3 shows a photograph of a spot of stimulated radiation at a distance of 10 cm from the emitting structure, as well as the intensity distribution for two mutually perpendicular directions. These results demonstrate a uniform, close to Gaussian, radiation intensity distribution profile. The angular divergence of stimulated radiation from the end of the structure is $\approx 15^\circ$ in the perpendicular direction to the plane of the structure and $\approx 18^\circ$ in the parallel direction.

Fig. 4 shows the emission spectra of $Al_2O_3/AlN/Al_{0.65}Ga_{0.35}N/AlN/Al_2O_3$ structures measured at the same optical pump power density $P_p = 150\,\text{kW/cm}^2$: spontaneous luminescence spectrum (*1*) and stimulated emission spectra (*2–5*). In the spectrum of stimulated radiation (*2*), detected normally to the chipped face, amplified components are observed. It also shows the components of stimulated radiation (*3, 4*) obtained with two orientations of the polarizer position: parallel and perpendicular to the surface of the heterostructure. The spectrum (*5*) of stimulated radiation of an asymmetric (single) structure $Al_{0.65}Ga_{0.35}N/AlN/Al_2O_3$ from Ref. [6] is shown for comparison.

Experimental dependences of the output radiation intensity on the pumping power density for $L = 1.5\,\text{mm}$ (Fig. 5) demonstrate threshold behavior, which confirms the formation of stimulated radiation at the pumping power density $P_p > 9\,\text{kW/cm}^2$. Fig. 6 shows the dependences of the intensity of stimulated radiation at two values of the optical pump power density depending on the length of the excitation zone L. The presence of amplification during radiation propagation in the $Al_{0.65}Ga_{0.35}N$ film confirms the exponential behavior of the curves when the values of L change. From the calculation for the dependences ofthe radiation intensities in the center of the λ_0 radiation line on L of the length of the amplifying region $I(\lambda_0, L) = \left(I_s s/g(\lambda_0)\right)\left(\exp[g(\lambda_0)L] - 1\right)$, where I_s is the luminescence power density, s is the cross-sectional area of the excited region [16,17], optical gain coefficients $g \approx 41.3$ and $21.6\,\text{cm}^{-1}$ can be determined for pumping power densities $P_p = 460$ and $150\,\text{kW/cm}^2$, respectively. An optical gain coefficient of $g \approx 2200\,\text{cm}^{-1}$ was obtained earlier in Ref. [4] for the film $Al_{0.65}Ga_{0.35}N$:Si by directly measuring the gain of the test radiation in the center of

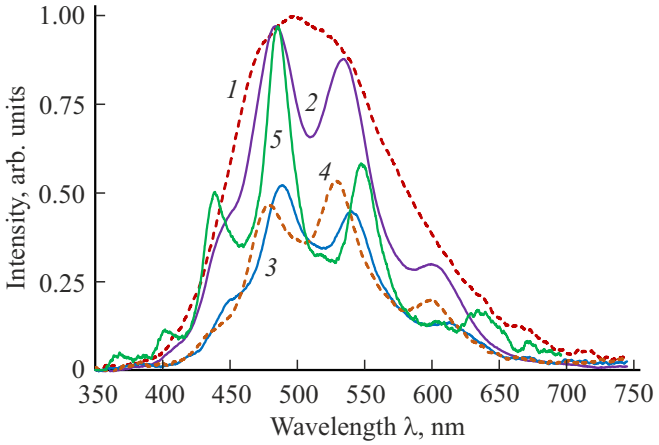


Figure 4. Emission spectra of heterostructures $Al_2O_3/AlN/Al_{0.65}Ga_{0.35}N/AlN/Al_2O_3$ (*1–4*) and $Al_{0.65}Ga_{0.35}N/AlN/Al_2O_3$ (*5*) at optical pump power density $P_p = 150\,kW/cm^2$: *1* — luminescence; *2, 5* — stimulated radiation, *3, 4* — *TE*- and *TM*-modes of stimulated radiation; *5* — results [6].

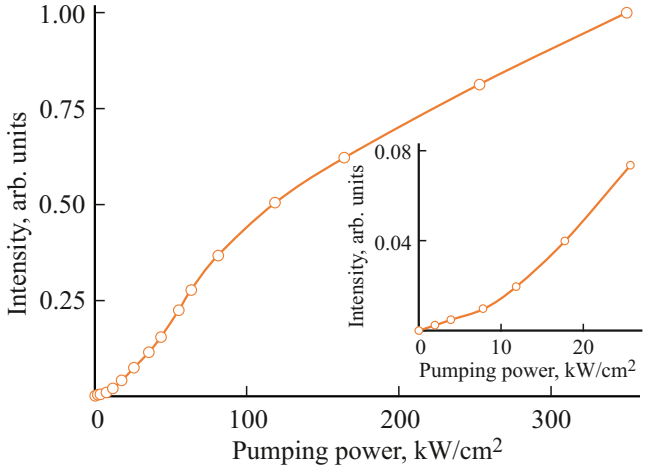


Figure 5. Dependences of the output radiation intensity on the power density of the optical pump P_p at the length of the excitation zone $L = 1.5$ mm. The box shows the initial region for the intensity of stimulated emission at P_p from 0 to 25 kW/cm^2.

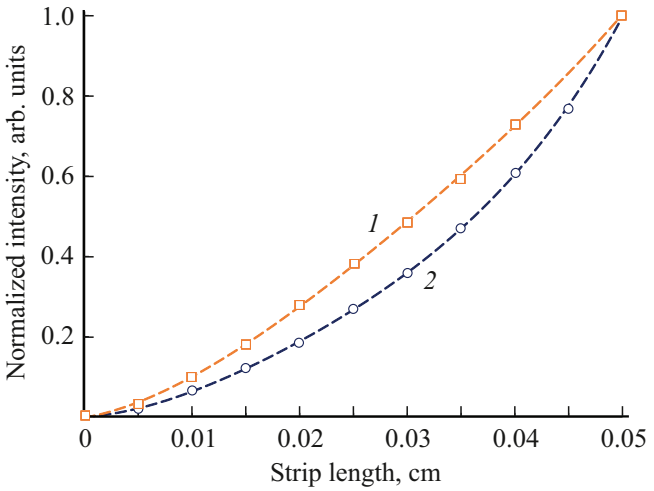


Figure 6. Dependence of the intensity of stimulated radiation on the length of the excitation zone L. $P_p = 220\,kW/cm^2$ (*1*) and $460\,kW/cm^2$ (*2*).

the radiation line with $\lambda_0 \approx 496.6$ nm at a pump power density of $P_p = 150\,kW/cm^2$. The significant difference in the values of g ($\sim 21.6\,cm^{-1}$) and [4] ($\sim 2200\,cm^{-1}$) is due to different measurement conditions. In the present case, the gain is measured in a planar waveguide, where part of the energy is lost due to radiation escaping through the side surfaces into the sapphire substrate (outflow modes). These losses lead to a decrease in the effective gain.

The quantum efficiency of converting pump energy at a power density $P_p = 150\,kW/cm^2$ into stimulated radiation energy was $\eta \approx 20\,\%$.

Two identical heterostructures $Al_{0.65}Ga_{0.35}N/AlN/Al_2O_3$ were used in the studied sample (Fig. 1), which consist of an $Al_{0.65}Ga_{0.35}N$ film with a refractive index of $n_1 \approx 2.17$ [18], an AlN buffer layer with $n_2 \approx 2.08$ [18] and a sapphire substrate with $n_3 \approx 1.776$ [19]. The external surfaces of the structure are in contact with air with $n_0 = 1$. In this case, the refractive indices meet the conditions $n_1 > n_2 > n_3 > n_0$, and, consequently, there are several critical angles of incidence of Θ radiation at the interface of the contacting media (Fig. 1) [20]. Radiation propagating from any point inside the $Al_{0.65}Ga_{0.35}N$-film experiences total internal reflection at angles of incidence exceeding a certain critical angle. At the boundary of $Al_{0.65}Ga_{0.35}N$-air is $\Theta_1 = \arcsin(n_0/n_1)$.

Calculations using Fresnel formulas [21] show that the reflection coefficient at the interface of the $Al_{0.65}Ga_{0.35}N$ film and the AlN buffer layer is small due to the insignificant difference between the refractive indices of these materials ($\sim 0.14\,\%$). In addition, the film thickness $h_1 \approx 360$ nm is less than the wavelength of luminescence. As a result, the radiation generated in the active layer of $Al_{0.65}Ga_{0.35}N$ effectively penetrates the AlN layer with minimal reflection losses. Therefore, the region consisting of an $Al_{0.65}Ga_{0.35}N$ film and an AlN buffer layer can be considered as a single optical waveguide. In such a system, two types of optical radiation can be distinguished: radiation propagating at small angles to the axis of the waveguide, which can exit the end of the heterostructure at angles of incidence less than $\Theta_1 = \arcsin(1/n_1) \approx 27^\circ$ (Θ_1 — angle relative to the normal to the end of the structure); radiation propagating at angles less than $\Theta_2 \leq \arcsin(n_3/n_1) \approx 58^\circ$ (Θ_2 — angle relative to the normal to the interface AlN — Al_2O_3) — flowing modes.

It can be seen from Fig. 4 that the width of the emission spectra increases with increasing thickness of the active excitation zone (curves *2* and *5*). This effect is explained by the fact that the number of supported optical modes increases in a thicker planar waveguide. Each of these

modes is characterized by its own spectral contribution, which leads to a broadening of the overall luminescence spectrum. In this case, a symmetrical planar waveguide selects certain transverse electric and magnetic modes from a wide range of luminescence, which leads to a narrower spectrum of stimulated radiation for these modes.

The values of the angles of total internal reflection at the boundary $Al_{0.65}Ga_{0.35}N$–Al_2O_3 are determined for the three main peaks in the experimental spectrum of stimulated radiation using the formula $\Theta = \arcsin(n_3/n_1)$ (Fig. 4, curve *2*) with wavelengths $\lambda_1 \approx 484.5$, $\lambda_2 \approx 534.1$ and $\lambda_3 \approx 599.2$ nm: $\Theta_1 = 54.19°, 54.28°$ and $54.42°$. The refractive coefficients for these wavelengths in the $Al_{0.65}Ga_{0.35}N$ film are $n_1 = 2.19, 2.18$ and 2.17 [19] and for sapphire $n_3 = 1.776, 1.770$ and 1.765 [20]. At $\Theta < \Theta_1$, there is no complete internal reflection from the walls of the waveguide, and the radiation partially leaves the waveguide through the boundary $Al_{0.65}Ga_{0.35}N/Al_2O_3$. As the Θ angle decreases, the proportion of radiation escaping from the waveguide increases due to refraction at the boundary, which reduces the gain.

The curves *3, 4* in Fig. 4 show that the radiation spectrum consists of a set of equidistant peaks, each of them consists of the sum of two flat *TE*- and *TM*-waves. The position of the equidistant peaks recorded in the experimental spectra is interpreted by the model presented in Ref. [20]. The radiation in a planar waveguide consists of the sum of two planar *TE*- and *TM*-waves. These waves propagate in the structure under study as in a planar waveguide due to reflection at the boundaries of the structure. For a light wave propagating in a dielectric layer, in addition to internal reflection, the condition of transverse resonance (or phase matching) must be fulfilled. This condition requires that the full phase shift of the phases in one complete zigzag (after two reflections from the upper and lower surfaces of the waveguide layer) was a multiple of 2π:

$$2kn_1h\cos\Theta + \delta_1 + \delta_2 = 2\pi m, \qquad (1)$$

where $k = 2\pi/\lambda$ is the wavenumber, h is the thickness of the waveguide, δ_1 and δ_2 are the phaseshifts that occur during total internal reflection at the boundaries of the waveguide, m is an integer that determines the mode order. Since the propagation of an electromagnetic wave in a waveguide is resonant, determined by the integer m, only certain discrete waveguide modes propagate in the studied structure. Each mode is characterized by its own spatial distribution of the field in the transverse direction, polarization, effective refractive index and angle Θ. Depending on the ratio of the refractive indices and the angle of incidence at the interface, the light wave can either channel into the waveguide layer or flow out into the substrate. It is possible to determine the angles of incidence Θ_2 at the boundaries in a planar waveguide from the equation (1) using known waveguide parameters. Due to the small calculated values of δ_1 and δ_2 [21], they can be ignored. The Goose–Hanchen effect [20] is not taken into account,

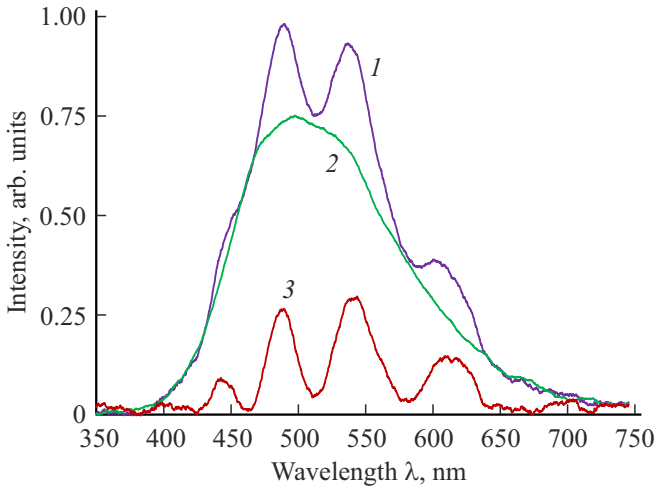


Figure 7. Stimulated emission spectra: integral (*1*), directional modes (*2*), resultant modes (*3*) at $P_p = 460\,\text{kW/cm}^2$.

since for its occurrence it is necessary to strictly fulfill the condition of total internal reflection at the boundary, which is not fulfilled for the resulting modes. For the total film thickness of $h_\Sigma \approx 2.2\,\mu$m, using the formula (1), the angles of incidence at the boundaries of $\Theta_2 = 52.6°, 51.7°$ and $50°$ and $m = 12, 11, 10$, respectively, can be calculated. Based on the experimental data obtained using the Fresnel formulas [21] for three peaks in the stimulated radiation spectrum (Fig. 4) with wavelengths λ_1, λ_2 and λ_3, values for the transmission coefficients through one plane of the waveguide $\sim$ 20, 28 and 38 %, respectively, were obtained.

Polarization measurements of the output radiation carried out using a Glan prism showed the presence of two groups of peaks in the spectrum with orthogonal linear polarizations and with different spectral positions. This situation is explained by the simultaneous propagation of *TE*- and *TM* modes with different effective refractive indices and different phase shifts in the waveguide. In this case, the radiation coming out of the end face of the structure turns out to be unpolarized. The cause of depolarization may be the superposition of several modes of different orders and the effects of diffraction and scattering on inhomogeneities at the end of the structure.

The contribution of various mechanisms for the output of stimulated radiation from a planar waveguide can be quantified. The method of analysis was as follows. Fig. 7 shows the integral spectrum of the stimulated output radiation $S(\lambda)$ (curve *1*) at the optical pump power density $P_p = 460\,\text{kW/cm}^2$. Since the shape of the stimulated emission spectrum in the studied medium with inhomogeneous spectrum broadening repeats the shape of the luminescence spectrum $L(\lambda)$, the following method was used to isolate the contribution of various modes. Based on the assumption that the shape of the spectrum from the end of the structure — the spectrum of directional modes

repeats $L(\lambda)$, the scaled luminescence spectrum $aL(\lambda)$ was subtracted from the full spectrum $S(\lambda)$. The a coefficient was selected in such a way that the intensity of the resulting $aL(\lambda)$ curve (curve *2*) at the edges of the spectral range ($\lambda \approx 380$ and 670 nm) was close to zero or turned to zero. Within the framework of this model, $aL(\lambda)$ corresponds to the radiation of guided modes exiting through the end of the structure, and the difference $R(\lambda) = S(\lambda) - aL(\lambda)$ corresponds to the radiation of the outgoing modes. The areas under the $R(\lambda)$ and $aL(\lambda)$ curves allow estimating the proportion of energy removed from the structure due to different mechanisms. The area under the $aL(\lambda)$ curve corresponds to the radiation of the guided modes. The area difference between the curves $R(\lambda)$ and $S(\lambda)$ corresponds to the emission of the outflow modes exiting through the lateral surfaces of the structure. It can be determined that $\sim 85\,\%$ of the total energy of stimulated radiation falls on the directed modes, and the remaining $\sim 15\,\%$ — on the resulting modes. For the same structure with a lower optical pumping power density $P_p = 150\,\text{kW/cm}^2$ (Fig. 4), the fraction of the end terminal is $\sim 80\,\%$. For comparison, a similar analysis performed for the asymmetric heterostructure $Al_{0.65}Ga_{0.35}N/AlN/Al_2O_3$ shows that this proportion is less and amounts to $\sim 60\,\%$. It can be concluded that the predominant mechanism of radiation output from the structures under study is output through the end of the waveguide associated with the propagation of guided modes.

The half-width of the emission spectrum of the resulting modes is $\Delta\lambda \approx 26\,\text{nm}$ (Fig. 7), which exceeds the instrumental resolution of the broadband spectrometer used ($\sim 0.5\,\text{nm}$). The high values for the half-width of the $\Delta\lambda$ radiation line may be due to several reasons.

The presence of changes in the thickness and composition of the layers of the heterostructure as they grow, which leads to spatial inhomogeneities in the refractive indices. This affects the spectral characteristics and can lead to its broadening.

The presence of roughness at the interface between the substrate and the film (the RMS roughness of the $Al_{0.65}Ga_{0.35}N$-film is less than 4.7 nm, for the sapphire surface less than 1 nm) leads to scattering of waveguide modes, which leads to a decrease in the intensity of stimulated emission and contributes to spectrum broadening.

The effect of the buffer layer. There is an AlN buffer layer with a thickness of $\sim 300\,\text{nm}$ between $Al_{0.65}Ga_{0.35}N$-film and the sapphire substrate. As a result, the physical interface between the two media is not a sharp geometric plane. Therefore, Fresnel's formulas, which are valid for ideal flat boundaries and monochromatic homogeneous waves, give an approximate description. For real broadband inhomogeneous electromagnetic waves, this can lead to deviations from the laws of geometric optics (violation of the law of internal reflection), especially near the critical angle, and contribute to broadening. However, the experimental data obtained are in good agreement with the models presented in this paper, which indicates the high quality of the studied $Al_{0.65}Ga_{0.35}N$-films.

It is possible to compare the radiation parameters of symmetric $Al_2O_3/AlN/Al_{0.65}Ga_{0.35}N/AlN/Al_2O_3$ and asymmetric $Al_{0.65}Ga_{0.35}N/AlN/Al_2O_3$ heterostructures [6]. Due to the fact that the thickness in the symmetrical structure is twice as large, favorable conditions are created for the effective propagation of a larger number of waveguide modes, including high-order modes. As a result, with the same pumping power, the output power of stimulated radiation for a symmetrical structure is 1.5 times higher. The structures differ in spectral composition and the prevailing radiation output mechanisms. In a symmetrical waveguide, a higher quality of the stimulated radiation output beam is observed. As can be seen from the comparison of Fig. 3, *b* of the present work and Fig. 4, *b* [6], its spatial intensity distribution becomes more uniform and closer to the Gaussian profile.

Conclusion

The results obtained demonstrate the promising use of highly alloyed symmetric heterostructures $Al_2O_3/AlN/Al_xGa_{1-x}N/AlN/Al_2O_3$ as effective broadband radiation sources in the visible and UV spectral regions (300−750nm). The totality of the obtained results demonstrates the stimulated nature of radiation with a low divergence value and a high quantum yield. The values of the optical gain coefficient up to $g \approx 41.3\,\text{cm}^{-1}$ measured in a planar waveguide at an optical pumping power density of $P_p = 460\,\text{kW/cm}^2$ show the possibility of creating effective broadband directional stimulated radiation emitters based on these structures. An important practical advantage is the ease of manufacturing symmetrical waveguides that do not require additional complex technological processes.

Funding

The work was performed within the framework of the state assignment FWGW–2025–0019.

Conflict of interest

The authors declare that they have no conflict of interest.

References

[1] J. Yang, K. Tian, C. Chu, Y. Zhang, K. Jiang, X. Sun, D. Li, X.W. Sun, Z.-H. Zhang. Advanced Electronic Materials, **11**, 2400247 (2025). DOI: 10.1002/aelm.202400247

[2] J. Hwang, W.J. Schaff, L.F. Eastman, S.T. Bradley, L.J. Brillson, D.C. Look, J. Wu, W. Walukiewicz, M. Furis, A.N. Cartwright. Appl. Phys. Lett., **81** (27), 5192 (2002). DOI: 10.1063/1.1534395

[3] P.A. Bokhan, N.V. Fateev, T.V. Malin, I.V. Osinnykh, Dm.E. Zakrevsky, K.S. Zhuravlev. J. Luminescence, **203**, 127 (2018). DOI: 10.1016/j.jlumin.2018.06.034
[4] P.A. Bokhan, K.S. Zhuravlev, D.E. Zakrevsky, T.V. Malin, N.V. Fateev. FTP, **57** 9), 731 (2023) (in Russian). DOI: 10.61011/FTP.2023.09.56987.5627
[5] P.A. Bokhan, K.S. Zhuravlev, Dm.E. Zakrevsky, T.V. Malin, I.V. Osinnykh, N.V. Fateev. Tech. Phys. Lett., **47** (14), 39 (2021) (in Russian). DOI: 10.21883/PJTF.2021.14.51186.18782
[6] P.A. Bokhan, K.S. Zhuravlev, D.E. Zakrevsky, T.V. Malin, N.V. Fateev. Opt. i spektr., **132** (9), 911 (2024) (in Russian). DOI: 10.61011/OS.2024.09.59189.6977-24
[7] I.V. Osinnykh, T.V. Malin, D.S. Milakhin, I.A. Aleksandrov, K.S. Zhuravlev. Avtometriya, **55** (5), 1 (2019) (in Russian). DOI: 10.15372/AUT20190513
[8] V.V. Ratnikov, M.P. Shcheglov, B.Ya. Ber, D.Yu. Kazantsev, I.V. Osinnykh, T.V. Malin, K.S. Zhuravlev. FTP, **52** (2), 233 (2018) (in Russian). DOI: 10.21883/FTP.2018.02.45448.8699
[9] A.V. Medvedev, A.A. Dukin, N.A. Feoktistov, V.G. Golubev. ZhTF, **86** (5), 118 (2016) (in Russian). DOI: 10.1134/S1063784216050169
[10] J. Valenta, I. Pelant, K. Luterova, R. Tomasiunas, S. Cheylan, R.G. Elliman, J. Linnros, B. Honerlage. Appl. Phys. Lett., **82** (6), 955 (2003). DOI: 10.1063/1.1544433
[11] K. Luterova, D. Navarro, M. Cazzanelli, T. Ostatnicky, J. Valenta, S. Cheylan, I. Pelant, L. Pavesi. Phys. Stat. Sol. C, **2** (9), 3429 (2005). DOI: 10.1002/pssc.200461206
[12] C. Shi, M. Liang, L. Wang, Y. Liu, W. Wang, S. Li. Opt. Lett., **50** (13), 4266 (2025). DOI: 10.1364/OL.565291
[13] Z.E. Lampert, J.M. Papanikolas, C.L. Reynolds. Appl. Phys. Lett., **102**, 073303 (2013). DOI: 10.1063/1.4793422
[14] K.S. Zhuravlev, I.V. Osinnykh, D.Y. Protasov, T.V. Malin, V.Yu. Davydov, A.N. Smirnov, R.N. Kyutt, A.V. Spirina, V.I. Solomonov. Phys. Stat. Sol. C, **10**, 315 (2013). DOI: 10.1002/pssc.201200703
[15] B.M. Ayupov, I.A. Zarubin, V.A. Labusov, V.S. Sulyaeva, V.R. Shayapov. J. Opt. Technol., **78**, 350 (2011). DOI: 10.1364/JOT.78.000350
[16] K.L. Shaklee, R.E. Nahory, R.F. Leheny. J. Lumin., **7**, 284 (1973). DOI: 10.1016/0022-2313(73)90072-0
[17] A. Oster, G. Erbert, H. Wenzel. Electron. Lett., **33**, 864 (1997). DOI: 10.1049/el:19970605
[18] D. Brunner, H. Angerer, E. Bustarret, F. Freudenberg, R. Hopler, R. Dimitrov, O. Ambacher, M. Stutzmann. J. Appl. Phys., **82**, 5090 (1997). DOI: 10.1063/1.366309
[19] I.H. Malitson. J. Optical Society of America., **52**, 1377 (1962).
[20] H. Kogelnik. IEEE Trans. Microwave Theory Tech., **23** (1), 2 (1975). DOI: 10.1109/TMTT.1975.1128500
[21] M. Born, E. Wolf. *Principles of Optics* (Pergamon Press, Oxford, 1975). DOI: 10.1016/0030-3992(75)90061-4

Translated by A.Akhtyamov